



Chemical Methodologies

journal homepage: <http://chemmethod.com>



Original Research article

Central Composite Design Optimization of Methylene Blue Scavenger using Modified Graphene Oxide Based Polymer

Mehrnaz Alem^a, Abbas Teimouri^{a*}, Hossein Salavati^{a*}, Shahnaz Kazemi^b

^a Department of Chemistry, Payame Noor University, 19395-3697, Tehran, Iran

^b Department of Chemistry, Birjand University, 97179-414, Birjand, Iran

ARTICLE INFORMATION

Received: 24 June 2017

Received in revised: 25 July 2017

Accepted: 20 August 2017

Available online: 30 August 2017

DOI: [10.22631/chemm.2017.49743](https://doi.org/10.22631/chemm.2017.49743)

KEYWORDS

Graphene oxide

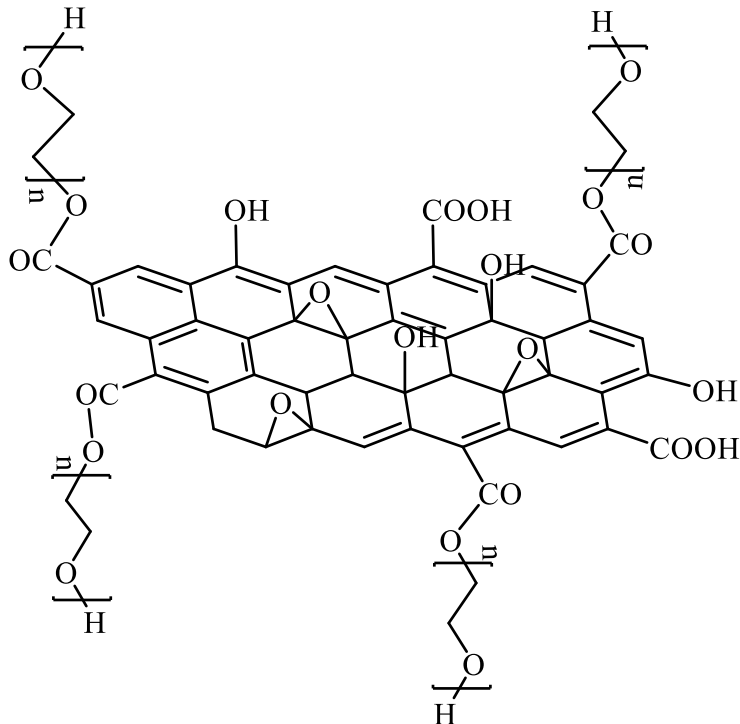
Polyethylene glycol

Nanocomposite

Photocatalytic.

ABSTRACT

This research reports the synthesis, characterization and catalytic properties of novel supported catalyst based on nickel acetate hydrate (denoted as NiOAC) immobilized on graphene oxide (denoted as GO) modified polyethylene glycol (abbreviated as PEG). The supported catalyst was characterized by X-ray diffraction spectroscopy (XRD), Scanning electron microscopy (FESEM), Fourier transforms infrared spectroscopy (FT-IR) and diffuse reluctance spectroscopy (DRS). In addition, under mild reaction conditions, the mentioned catalyst exhibited high photocatalytic activity and reusability in photocatalytic degradation of dyes as pollutants. For this research, a statistical method called Response Surface Methodology (RSM) has been used to economize the number of experiments and their meaningful interpretation. The effect of various factors such as catalyst amount, time, pH on degradation of methylene blue were investigated. Optimization results for 20 ppm methylene blue showed that maximum degradation efficiency 92.9% was achieved at the optimum conditions: catalyst amount 24.6 mg, pH= 7.6 and time 23.3 min.

Graphical Abstract

Structure of synthesized PEG grafted graphene oxide.

Introduction

Graphene oxide (GO) with a layered structure is characterized by functional groups on the surface such as carboxyl, hydroxyland epoxide. GO shows extraordinary unique properties such as strong mechanical strength, exceptional thermal properties, high ratio of surface area ($2630\text{ m}^2/\text{g}$), etc [1]. Graphene-based materials with various types of functionalization are available, and they have unique properties including charge transportation, electrical conductivity, mechanical strength, and porosity [2]. Graphene oxide nanosheets decorated mostly with functional groups such as epoxide, carboxylic and hydroxyl groups. GO nanosheets have hydrophilic properties due to the wide range of functional groups containing oxygen on the surface of layers of graphene oxide. These functional groups allow graphene oxide nanosheets to be no covalently functionalized by bio molecules, carbon nanotubes, organic molecules and by p-stacking interactions, hydrogen bonding interaction or vander waals forces [3-9]. Graphene oxide nanosheets is readily functionalized with various surfactants, polymeric materials, and nanoparticles in order to provide enormous potential for applications in materials science and engineering [10, 11]. In recent years, graphene oxide catalyzed photocatalytic reactions such as degradation of dyes [12-16]. Graphene oxide is prepared

by the oxidative procedure of graphite by one of the principle methods improved by Brodie, Hummers or Staudenmeir [17]. Functionalization of graphene oxide can fundamentally change graphene oxide's electrical, mechanical, thermal and electrical conducting properties, also sulfated graphene was tested as catalyst for the esterification of acetic acid, the Beckmann condensation and hydration of propylene oxide. In addition, some reports have demonstrated that immobilizations of transition metal nanoparticles on graphene oxide nanosheets produce efficient photocatalysts [18-21]. Graphene-based polymer composites have the unique mechanical, electrical and flame retardant properties, compared to the neat polymer. Also, surface to volume ratio of graphene is higher than carbon nanotubes, rendering graphene potentially more favorable to form functional nanocomposites for various applications. It was also shown that the developments in mechanical and electrical characteristics of graphene-based polymer composites are much better in comparison to that of clay or carbon filler based polymer composites [22-26]. Polyethylene glycol has the ability to serve as active sites since the polyethylene oxide chains can form stable complexes with metal cations, similar to crown ethers. To maintain electro neutrality, such PEG-metal cation complexes must bring an equivalent anion into the organic phase, thus making the anion available for reaction with the organic reactants. Many factors affect phase catalytic activity, such as, chain end effects, polyethylene glycol molecular weight and the nature of the associated cations and anions [27, 28]. Design-expert 7.0.0 software (Stat Ease, USA) was used for this study. In this study, central composite design (CCD) was employed with 30 experiments. Artificial neural network (ANN) was used for designing the process modeling [29]. Formal batch adsorption studies depend on different process parameters, such as initial solution pH, time and catalyst amount. But, this approach does not determine the combined effect of all the process parameters. For scale-up studies, conventional batch process is time consuming and to determine the optimum levels (which may be unreliable) requires a large number of experiments and thereby, increase the overall cost of the process. Thereupon, The main aim of the present study is to consider a novel system for catalytic and photocatalytic properties by using nickel acetate, immobilized over graphene oxide modified with polyethylene glycol as natural molecule. The advantage of this catalyst is that we combine the high surface area of the graphene oxide support for immobilization of catalytic active metal ions as heterogenous catalyst with the polyethylene glycol as a carrier of functional and oxygen groups for link to metal ions and create the active sites. In addition, we describe the photocatalytic activity of the catalyst and photodegradation by visible light irradiation of dyes as pollutants using a synthesized photocatalyst with two components, GO and PEG as environmentally

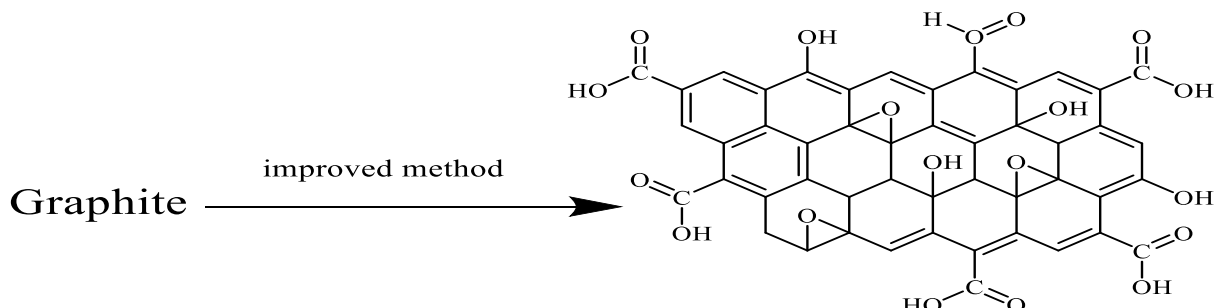
friendly and nickel acetate as owing to have vacant d orbitals forexciting the electron for electron transfer reactions.

Materials and methods

Solvents, reagents and chemicals were obtained from Merck, Fluka or Aldrich chemical companies. The samples were ground into a fine powder for characterization. FT-IR spectra were obtained as potassium bromide pellets in the range of 400-4000 cm⁻¹ with a Nicolet-Impact 400D instrument. Field emmision scanning electron microscopy (FESEM) of the catalysts and supports were taken on SEM Philips XL 30 instrument. Diffuse reflectant spectroscopy (DRS) UV were recorded on a 160 Shimadzu spectrophotometer. X-ray diffraction (XRD) patterns were recorded with a Philips X-ray diffractometer (Model PW1840).

Preparation of graphene oxide (denoted as GO)

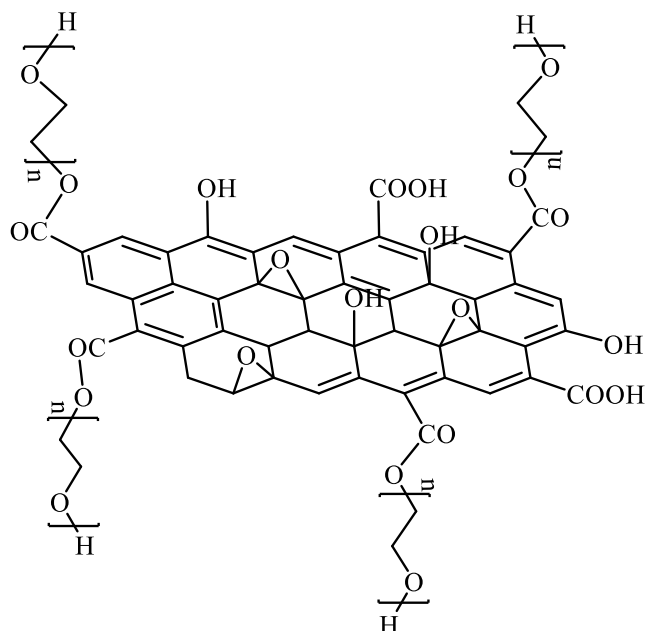
For the improved method, a 9:1 mixture of concentrated H₂SO₄/H₃PO₄ (360:40 mL) was added to a mixture of graphite powder (3.0 g, 1 wt equiv) and then KMnO₄ (18.0 g, 6 wt equiv) was added slowly to the resultant mixture, producinga slight exotherm to 35-40 °C. The reaction was then heated to 50 °C and stirred for 12 h. The reaction was cooled to room temperature and poured onto ice (400 mL) with 30% H₂O₂ (3 mL). The mixture was centrifuged (4000 rpm for 4 h), and the supernatant was decanted away. The remaining solid material was then washed with 200 mL of water, 200 mL of 30% HCl, and 200 mL of ethanol and centrifuged under 4000 rpm for 4 h and the supernatant decanted away. The material remaining after this extended, multiple-wash process was coagulated with 200 ml of ether and the resulting suspension was filtered over a PTFE membrane with a 0.45 pore size. The solid obtained on the filter was vacuum-dried overnight at room temperature, obtaining 5.8 g of product [17]. Scheme 1 shows the structure of the resultant graphene oxide.



Scheme 1.Structure of synthesized graphene oxide.

Preparation of polyethylene glycol-grafted graphene oxide (denoted as PEG-GO)

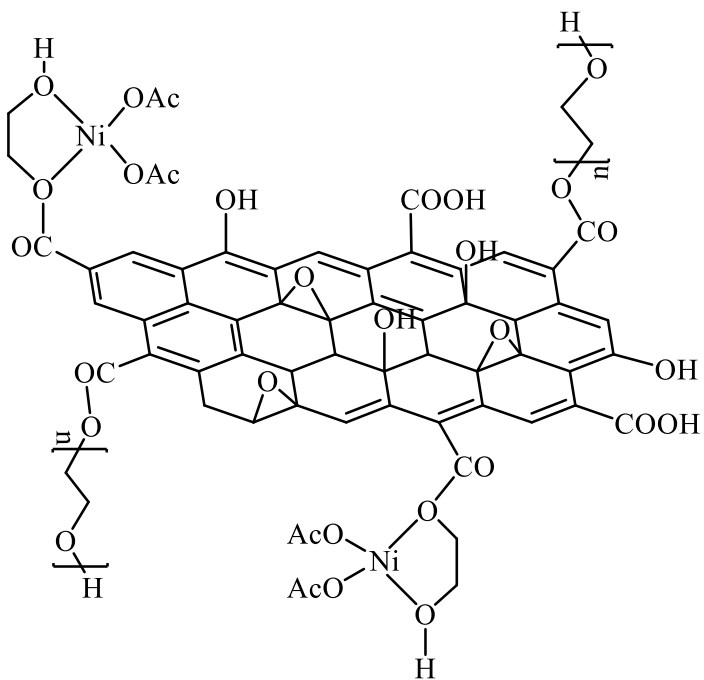
The PEG-modified GO polymeric nanocomposite was prepared through a covalent bond formation between a polymeric chain of polyethylene glycol and graphene oxide which was called PEGylation. Accordingly, 0.05g graphene oxide was dissolved in the minimum possible amount of deionized distilled water and then was exposed to ultrasonic for 5 min. After removing the solution from the ultrasonic bath, 2 ml of solution was immediately added to 1g polyethylene glycol 600. The mixture was stirred under 300 rpm for 24 h at 25 °C. After a certain time, the obtained modified graphene oxide was completely dissolved in the hydrophilic polymer. Scheme 2 shows the structure of the resultant composite [30].



Scheme 2. Structure of synthesized PEG grafted graphene oxide.

Preparation of supported catalyst with nickel acetate salt (denoted as NiOAC@PEG-GO)

The supported catalyst was synthesized by ultrasonic irradiation method, in this way 0.1g PEG-GO was dispersed in ethanol under ultrasonic irradiation for 30 min (solution 1) after that we prepared solution of nickel acetate in ethanol by dispersion of 0.05 g simple nickel salt (solution 2), then added solution 2 to the solution 1 under ultrasonic irradiation for 30 min. The obtained mixture, stirring for 12 h at 60 °C under magnetic stirring after that centrifuged and dried in air. Scheme 3. Structure of synthesized graphene oxide.



Scheme 3. Proposed scheme for the structure of supported catalyst.

Result and discussion

Sample characterization

Figure 1 shows the FT-IR spectra of prepared materials and the following functional groups were identified in all samples: (3300-3400 cm⁻¹) related to O-H stretching vibrations, (1720-1740 cm⁻¹) subjected to C=O stretching vibration, characteristics band for C=C from unoxidized sp² C-C bonds appeared in (1590-1628 cm⁻¹), and C-O vibrations appeared at 1228 cm⁻¹ and for Epoxide groups at (849, 1048 cm⁻¹) ranges. A band at 1114 cm⁻¹ corresponds to the stretching vibration of O-C-O group, which is a characteristic peak for polyethylene glycol skeleton (as shown in figure 1c). The pristine graphite typify the characteristic band at 3430 cm⁻¹ for O-H stretching and at 1610 cm⁻¹ for skeletal vibrations from graphitic domains of adsorbed water and aromatic domain (C=C), respectively (Figure 1a). Some new peaks at 1726 cm⁻¹ for C-O stretching appeared for graphene oxide, 3447 cm⁻¹ for O-H stretching, and 1048 cm⁻¹ and for C-O stretching from that of pristine graphite. The C-C aromatic peak shows characteristic peak at 1621 cm⁻¹ GO due to the presence of some electron-withdrawing oxygen-containing functional groups [17]. the case of functionalization of GO with PEG the -OH stretching peaks (3447 cm⁻¹) of GO are shifted to lower energy vibration at 3443 cm⁻¹ for GO-PEGnanocomposite (containing 3 wt% GO) suggesting the H-bonding interactions

between PEG and GO sheets. The 1726 cm^{-1} peak of C-O group shows a shift to 1649 cm^{-1} and the epoxide stretching vibration of GO at 1048 cm^{-1} has shifted to 1114 cm^{-1} indicating H-bonding between PEG and epoxy group of GO. The increased frequency of vibration is due to the ring structure of H-bonded epoxy group of GO in the GO-PEGnanocomposites [17-30]. After immobilization of acetate nickel on PEG-GO the broad new peak appear at 1557 cm^{-1} was related to acetate group and confirmed the simple salt of nickel was supported on PEG(Fig.3d). the peak related to Ni-O bond was observed below 1000 cm^{-1} ranges.

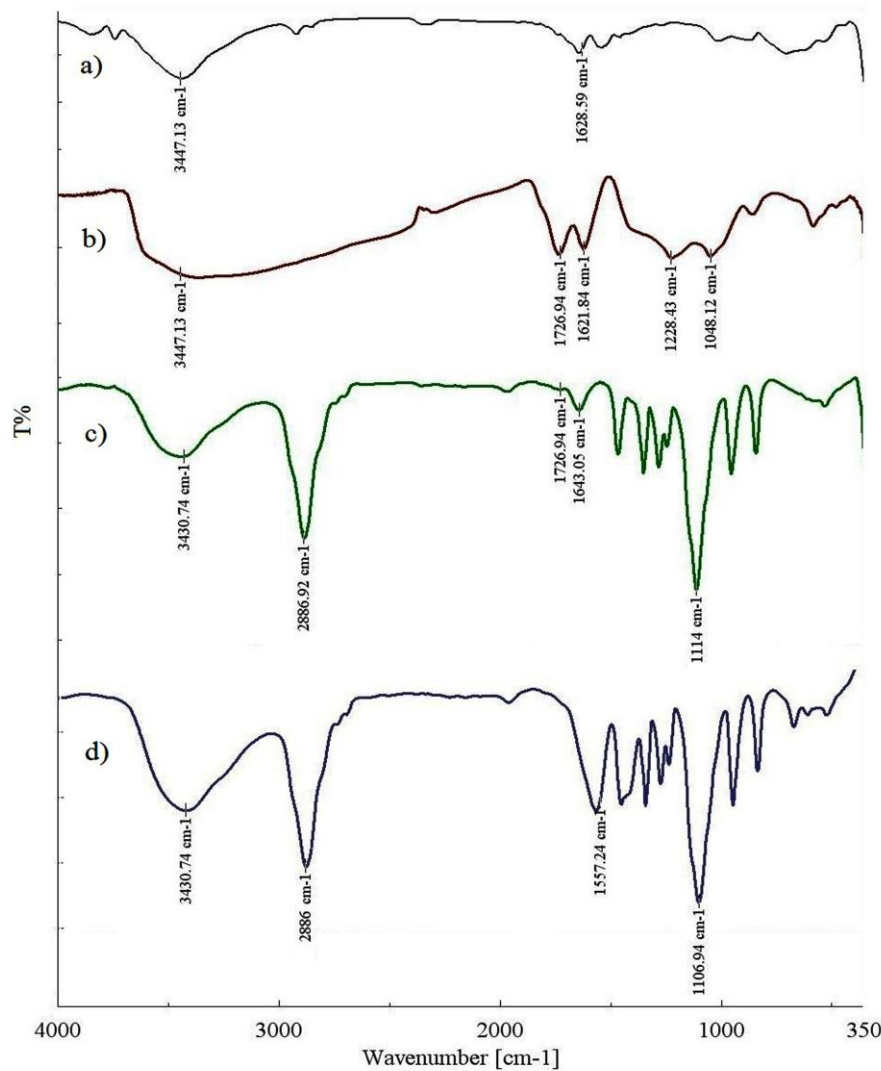


Figure 1. FTIR spectrum of a) graphite b) GO, c) PEG-GO, d) NiOAC@ PEG-GO.

Diffuse reflectance (DR) Uv spectra of GO, PEG-GO and NiOAC@PEG-GO was studied. Figuren 2a shows DR Uv spectrum of graphene oxide. The UV spectra of GO showed absorption bands in the

227-231 nm regions as previously reported for GO due to The $\pi\rightarrow\pi^*$ transitions [17]. For PEG-GO the peak related to GO was observed and confirmed that GO was present in PEG-GO, in addition the peak subjected to C-O band for polyethylene glycol was observed at 380-400 nm regions(Figure 2b).For supported catalyst the bands for nickel acetat (due to d \rightarrow d transitions)were observed with the shift due to supported nickel acetate salts on polyethylene glycol grafted graphene oxide(figure 2c).

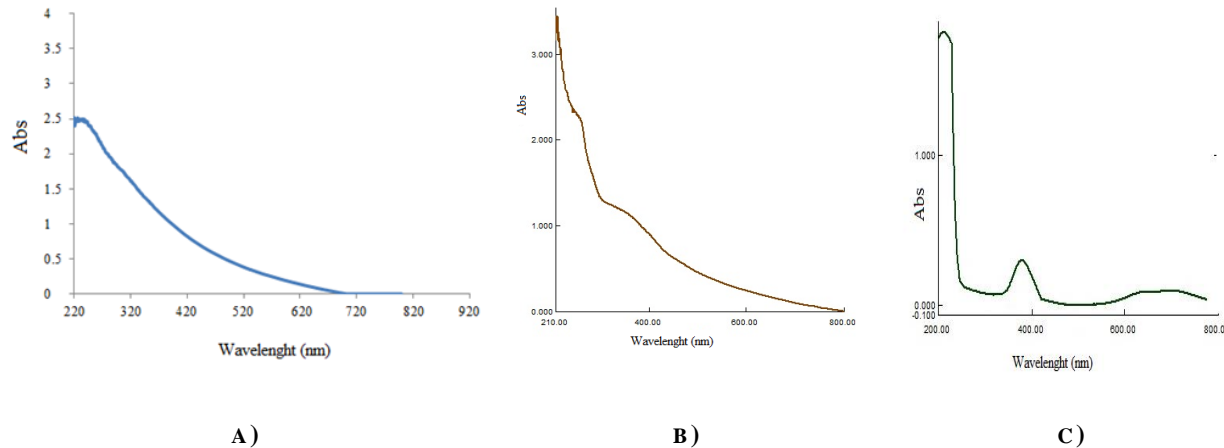


Figure 2. DR Uv-vis spectra of a) GO, b) PEG-GO, c) NiOAC@ PEG-GO

To investigate the effect of the modification procedure on the surface morphology, the surface FESEM images were prepared and then were compared together in Figure 3.To investigate the effect of the modification procedure on the surface morphology, the surface FESEM images were prepared and then were compared together in Figure 3. The FESEM images of GO are also shown in Figure 3a. In Figure 3a the morphology of GO was shown layers with about 100 nm thickness. PEG supported on the surface of graphene oxide and formed polymer thin layer on the top of the GO (Figure 3b). As can be seen, the surface morphology was changed by supporting the PEG which led to the creation of a smoother and more compressed surface than that of unmodified GO.Figure 3c shows that the surface morphology was changed by supporting the nickel acetate which led to the disappear smoother and compressed surface than that of unmodified graphene oxide grafted polyethylene glycol.

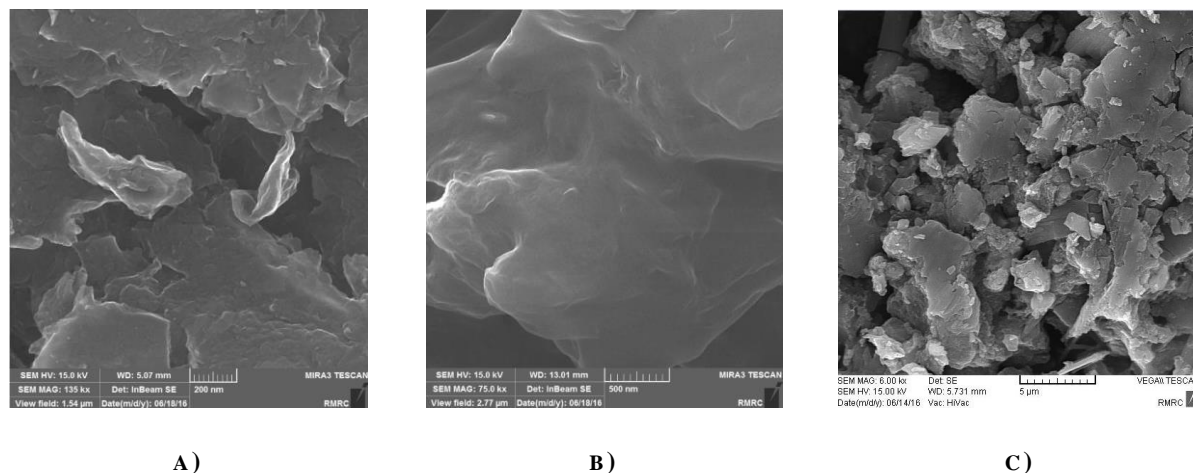


Figure 3. FESEM images of a) GO, b) PEG-GO, c) NiOAC@ PEG-GO.

Figure 4 was shown XRD patterns of NiOAC, GO, PEG-GO and NiOAC@ PEG-GO. XRD pattern for nickel acetate hydrate shows monoclinic structure with compare to XRD laboratory [31].The two-theta position of the (001) GO diffraction peak can show a range of $\sim 7\text{-}12^\circ$ two theta (Cu K α radiation) depending on the amount of residual water intercalated between basal planes in a GO film. In addition, there is a broad peak at $\sim 19^\circ$ two theta due to a unoxidized component(s) generated during the chemical processing of bulk graphite powder to make graphene oxide nanosheets [14]. After modification of GO with PEG the XRD pattern of GO-PEG was shown two characteristic peaks of PEG according to previous reported and confirming the immobilization of PEG on GO nanosheets. Immobilization of nickel acetate on the surface of GO-PEG led to change in the powder XRD pattern when compared with that for GO-PEG is confirming the formation of a new material and a possible change in crystallinity and interplanar space. From XRD images for the supported catalyst, the characteristics peaks for the monoclinic structure of nickel acetate was maintained after immobilization of nickel acetate and the peaks at $2\theta=13.2$ and 28.5 for monoclinic structure of nickel acetate was observed for XRD pattern of the catalyst.

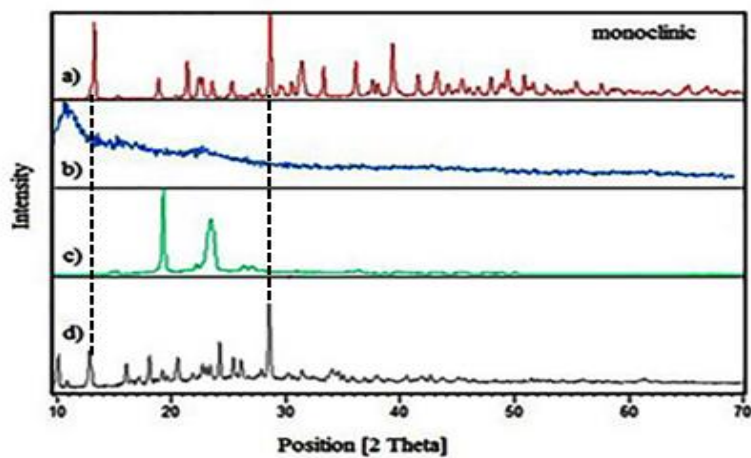
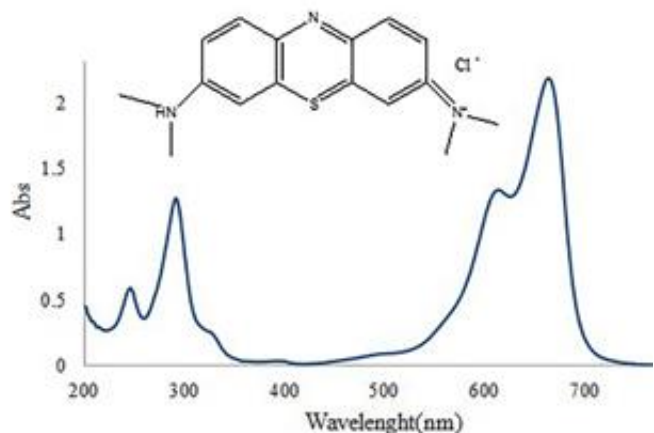


Figure 4. XRD images of a) NiOAC b) GO, c) PEG-GO, d) NiOAC@ PEG-GO.

Degradation of methylene blue (MB)

Methylene blue was selected as model dye for investigation of photocatalytic degradation of dyes as pollutants. Methylene blue is a heterocyclic aromatic chemical compound with the molecular formula C₁₆H₁₈N₃SCl. At room temperature it appears as an odourless green powder, which yields a blue solution when dissolved in water and gives characteristic spectrophotometric absorbance at 663 nm. It has many applications in the various fields. Methylene Blue (MB) is a cationic dye, extensively used in variety of industrial application with main applications in coir and textile industries. It is most commonly used dye for coloring cotton, wood, paper stocks, and silk. It is also utilized in the field of medicine [25]. Scheme 1 shows the structure and spectrum of MB.



Scheme 4. Structure and UV-vis spectrum of methylene blue.

The photocatalytic reactions were performed for 20 ppm initial concentration of MB under different experimental conditions, using different amounts of catalyst, time and various pH for degradation of methylene blue; this was done without irradiation, and the pH conditions were changed from acidic to basic. For consideration of effect of immobilization of supporting procedure on photocatalytic activity the experiments under same conditions was performed with NiOAC as catalyst. The results showed even up to 1h the degradation of methylene blue was trace in the presence of NiOAC and PEG as catalyst, so the influences of supporting NiOAC on the surface of graphene oxide and on the photocatalytic degradation of MB were obvious (Figure 5, Figure 6).

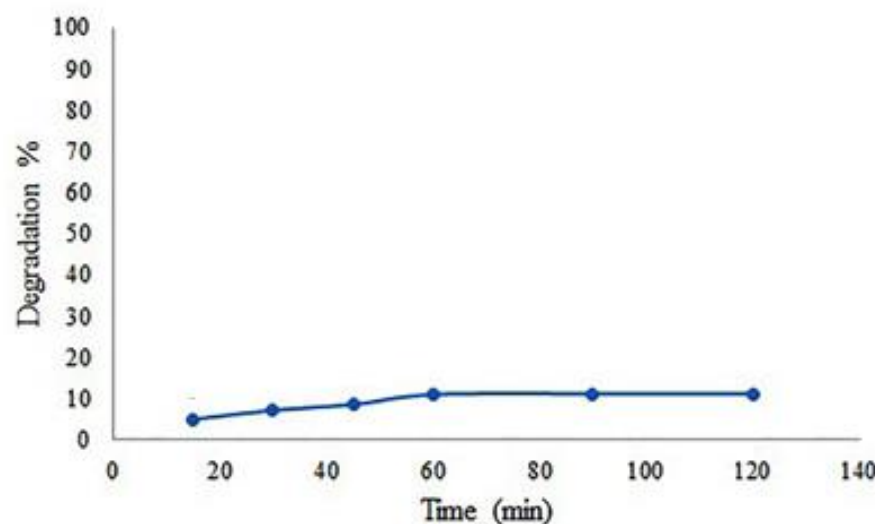


Figure 5. Degradation of methylene blue with NiOAC as catalyst, $C_0=20$ ppm.

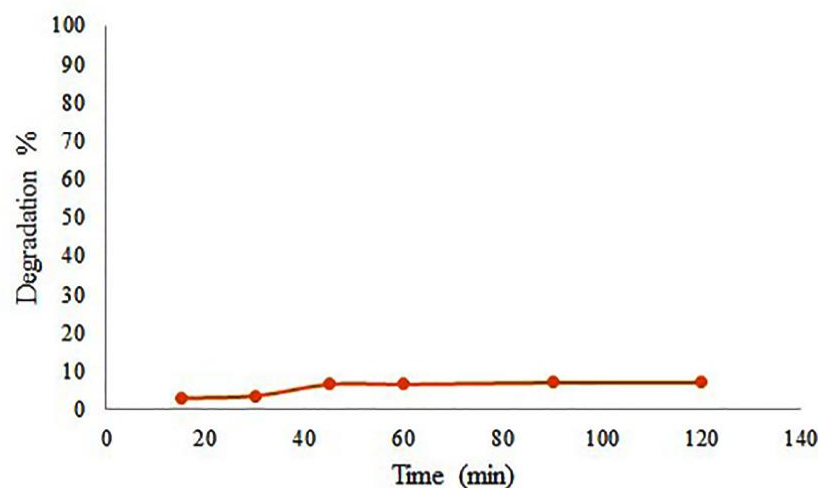


Figure 6. Degradation of methylene blue with PEG as catalyst, $C_0=20$ ppm.

The design expert 7.0.0 software was used for regression analysis of the data obtained and to estimate the coefficient of the regression equation. The equations were validated by the statistical tests called the ANOVA, to determine the significance of each term in the equations fitted and to estimate the goodness of fit in each case. Response surfaces were drawn for the experimental results, obtained from the effect of different variables on the percentage removal of dye, in order to determine the individual and cumulative effects of these variables and the mutual interactions between them. The small values of coefficient of variation (C. V. %) and standard deviation (Std. Dev.) indicated reliability. The small anticipated residual sum of squares (PRESS) is a criterion of how good the model fits each point in the model. The smaller the PRESS statistic, the better the model fits the data points. The above results indicating that, the proposed quadratic model guarantees a precise demonstration of the experimental data as well as indicated high validity and adequacy of model in predicting the degradation percentage of methylene blue. The Fisher's F value with a low probability ($p < 0.0001$) showed that the model was significant. The multiple correlation coefficient (R^2) demonstrated the goodness of the model. Moreover, R^2 value is 0.938 could be explained by the developed quadratic model, and the predicted R^2 values were in agreement with adjusted R^2 , which means all the terms depicted in the model were significant. In this case, the non-significant lack-of-fit (0.07) confirmed the quadratic model was valid for this process.

Comparison between theoretical and experimental data

The CCD equation of actual factors was solved by partial differential calculus for obtaining the optimum value of A, B, C. The optimized value showed below and Table 1 shows optimized data was obtained for this study. A (pH)=7.6, B (catalyst amount)=24.6 mg, C (time)=23.3 min for initial concentration 20 ppm. For optimized condition, the experimental percentage of degradation was 92.9%.

Table 1. Constraints applied for optimization process for initial concentration 60 ppm.

CATALYST AMOUNT	TIME	PH	REMOVAL%
24.6 MG	23.3 MIN	7.6	92.9

The regression plot of the trained network was shown in Figure 7. The trained network gave a correlation coefficient of 0.938. A high correlation coefficient of this plot signified the reliability of the neural model with the experimental data.

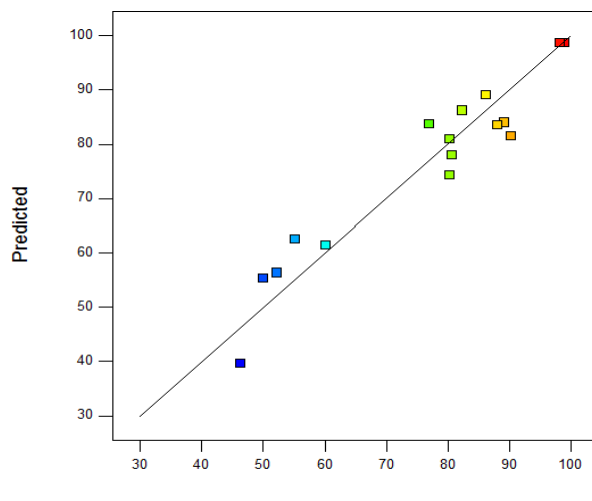


Figure 7. Regression plot (experimentally vs. predicted).

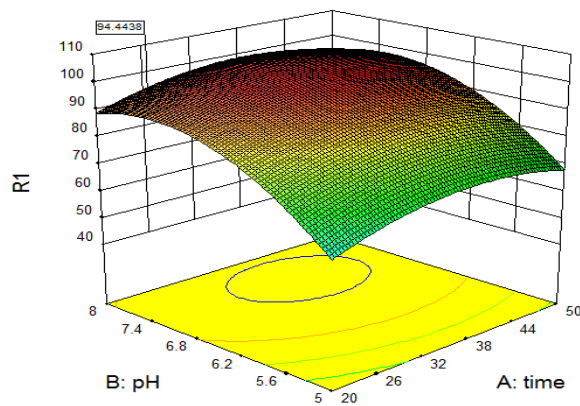
The model summary Statistics results was showed in Table 2. The predicted R-squared of 0.892 is as close to the adjusted R-squared of 0.796. This confirmed your model is acceptable.

Table 2. Model Summary Statistics.

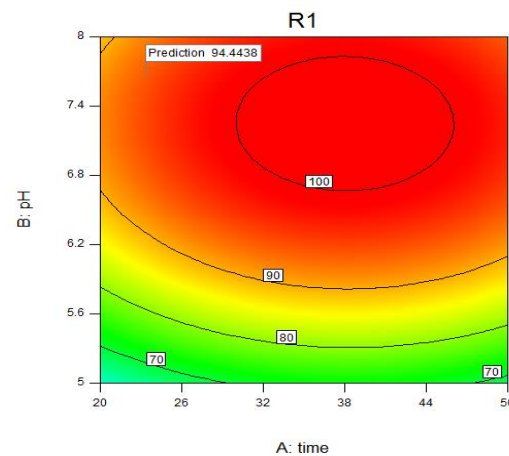
Source	R-Squared	Adjusted R-Squared	Predicted R-Squared
Quadratic	0.938	0.796	0.892 Suggested

The combined effect of different levels of initial solution pH and time on MB degradation using the keggin polyoxometal supported on modified graphene oxide can be predicted from the contour plot as shown in Figure 8a. From the contour plot, it can be observed that MB degradation percentage increased with increase of time and pH. Solution pH affected the chemistry of the degradation of MB, the activity of pH the adsorbent surface, as well as competition degradation of MB for the binding sites. The optimized pH and time were 7.6, 23.3 min. The combined effect of catalyst amount and contact time on dye degradation was shown in the contour plot of Figure 8c. The percentage of MB degradation increased by increased with catalyst amount. The rate of dye degradation was increased with enhancing the amount of catalyst. This could be due to the increase in the exposed surface area of the catalyst. However, it must be noted that after a certain limit (24.6 mg), if the amount of catalyst had been increased further, there would have been a saturation point. Both the number of active sites on photocatalyst and the penetration of light through the suspension are influence by the amount of photocatalyst. The increase in the loading of photocatalyst can increase the rate of the deactivation of activated molecules by collision with the ground state photocatalyst. From the results it was observed that a maximal degradation efficiency of 92.9% was achieved at 24.6 mg catalyst amount and 23.3 min of time. The combined effect of

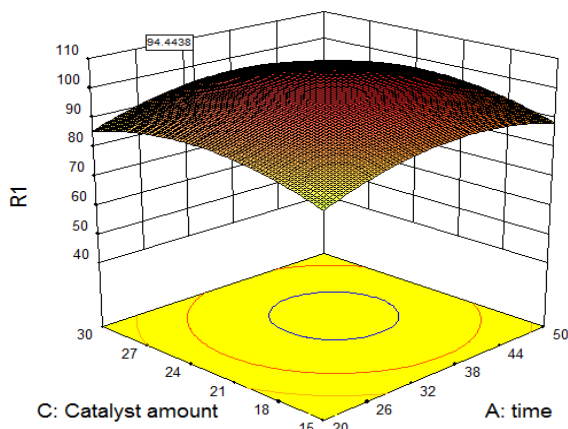
catalyst amount and pH on MB degradation was shown in Figure 8e. The percentage of MB degradation increased by increased with catalyst amount. Higher catalyst amount enhanced the catalytic active sites force and increased the MB adsorption. From the results it was observed that a maximal degradation efficiency of 92.9% was achieved at optimized pH and catalyst amount were 7.6, 24.6 mg.



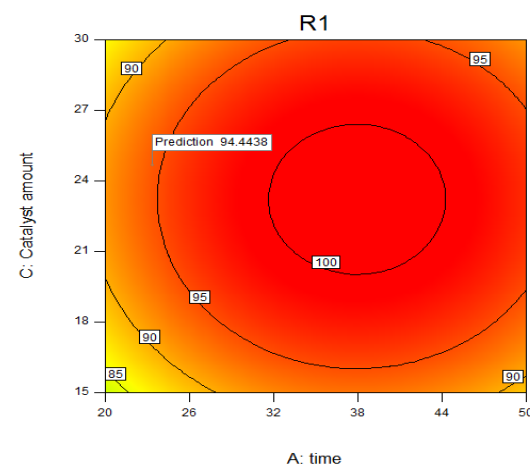
a)



b)



c)



d)

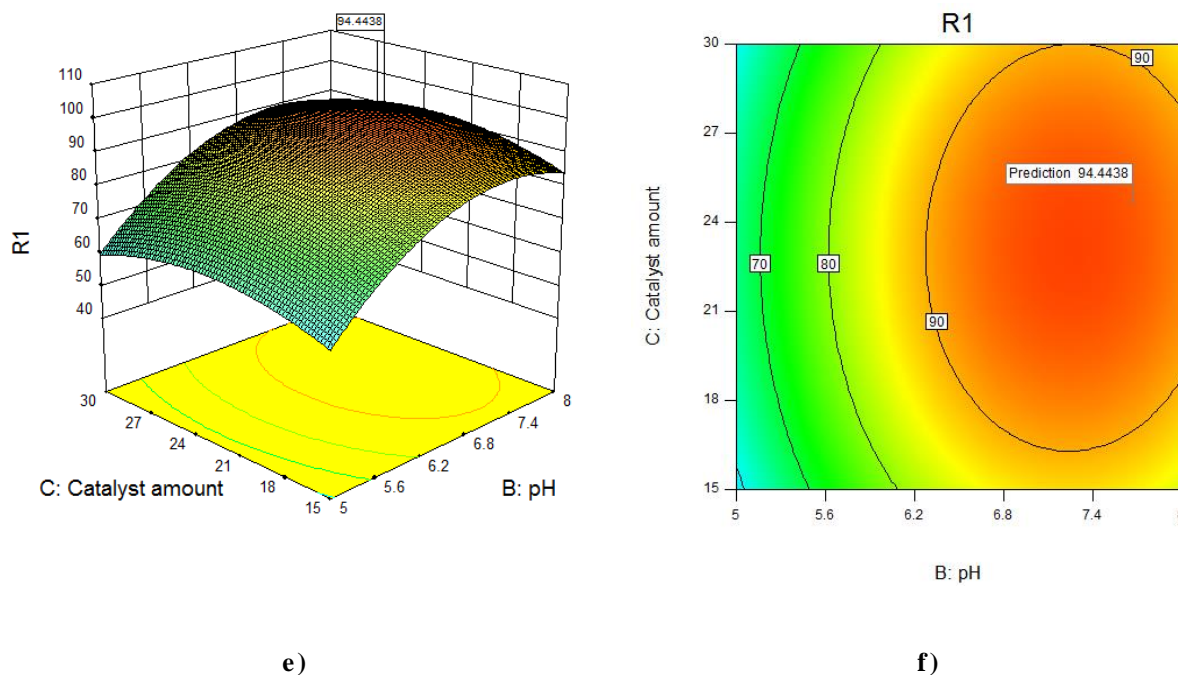


Figure 8. Three dimensional response surface graph for the degradation of MB wastewater (a) % MB degradation versus time and pH (b) counter plots for pH and time, c) MB degradation versus catalyst amount and time, d) counter plots for catalyst amount and time, e) MB degradation versus the catalyst amount and pH, f) counter plots for pH and catalyst amount, all experiments were performed for initial conc=20 ppm.

Catalytic behavior, separation and recyclability

The stability of the supported catalyst was monitored using multiple sequential degradation of MB with synthesized catalyst under visible light irradiation. For each of the repeated reactions, the catalyst was recovered, washed thoroughly with water and dried before being used with fresh methylene blue solution. Figure 9 shows that the catalysts were consecutively reused five times. The catalyst was recovered for five runs without the loss of activity.

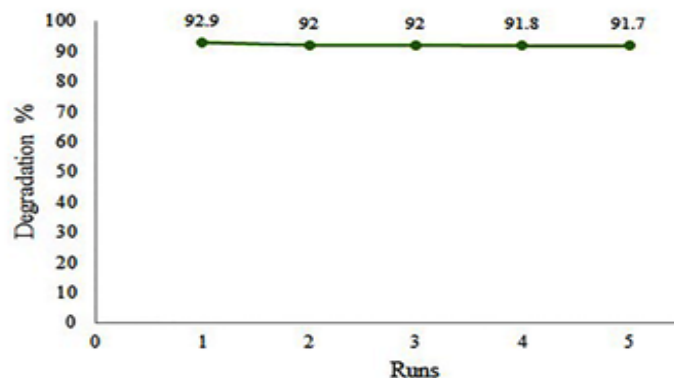


Figure 9. Reusability of catalyst in degradation of MB with synthesized catalyst

For considering the effect of methylene blue concentration on the photocatalytic activity, the experiments were performed under optimized conditions which obtained from CCD experiments at 7 different dye concentrations (20, 30, 50, 60, 80, 100, 150). Figure 10 shows that percentage degradation by catalyst is decreased by increasing the initial dye concentration from 20 to 150 mg/L and pH=7.6. The reduction of degradation by raising the dye concentration can be explained by the decrease in active sites on the adsorbent surface due to aggregation of particles. In addition, after 150 ppm the degradation was nearly constant. The effect of initial dye concentration on degradation showed in Figure 10.

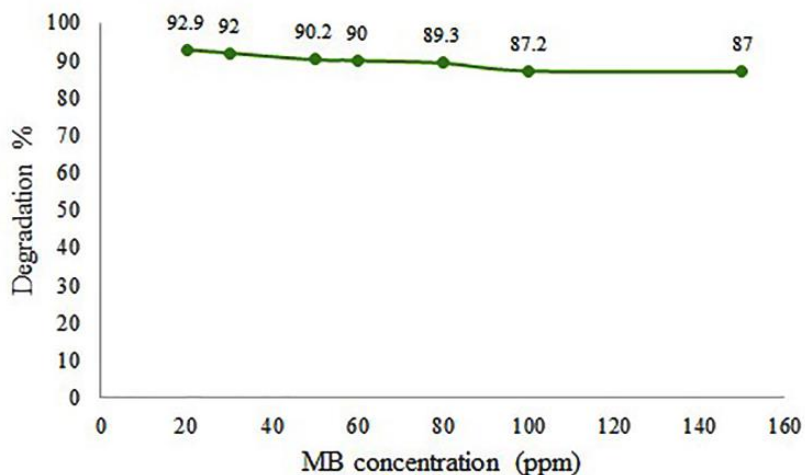


Figure 10. Effect of initial concentration of dye on the photocatalytic degradation of methylene blue under optimized condition, $C_0=x$ ppm.

For investigation of the catalyst was intact after photo catalytic reaction the FT-IR spectrum of catalyst after reused was taken and the results showed the peaks at 1105 cm^{-1} , 1569 cm^{-1} , 1720 cm^{-1} , 2924 cm^{-1} , 1444 cm^{-1} and 3400 cm^{-1} corresponding to the supported catalyst was remained after reused with shift due to degradation procedure (Figure 11). Many investigators have suggested various mechanisms for the degradation of dyes as pollutants. To exposure to visible light irradiation, the metal salts excited by light to give exited electron. This excited state will provide an electron in the conduction band leaving a hole in the valance band. This electron is then trapped by molecular O_2 forming O_2^- ions. The valance band hole generates hydroxyl radical from hydroxyl ions which can easily attack the adsorbed dye, thus leading finally to their complete mineralization. Scheme 4 suggests the photocatalytic degradation pathways.

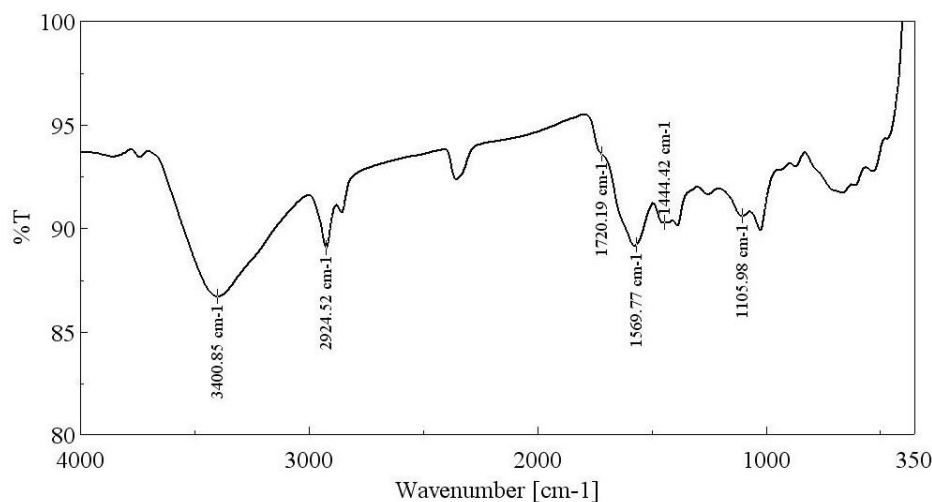
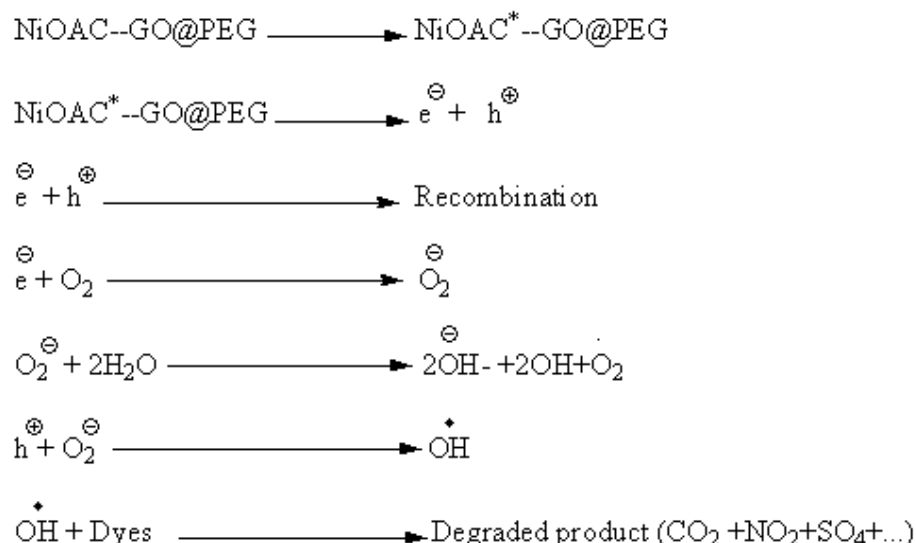


Figure 11. FT-IR spectrum of reused catalyst after degradation of MB



Scheme 4. Proposed mechanism for excitation of electron in degradation of dyes by supported catalyst

Table 3. compares the photocatalytic activity of the supported catalyst with those of other reported catalysts for the degradation of dyes.

Table 3. Comparison of reaction data for the present method in degradation of dyes and other reported methods.

CATALYST	DYES	REF
NiOAC@ PEG-GO CuO@GO	METHYLENE BLUE METHYL ORANGE	THIS WORK 32
Ag ₃ PO ₄ @GO	METHYLENE BLUE	13
TiO ₂ @RGO	ORGANIC DYES	14
TiO ₂ @GO	METHYLENE BLUE	15
Fe ₃ O ₄ @RGO@TiO ₂	ORGANIC DYES	16

Conclusions

NiOAC-supportedmodified graphene oxide (denoted as NiOAC@ PEG-GO) was prepared by anchoring NiOAC on the surfaces of PEG-coated GO nanoparticles. This catalyst showed excellent photocatalytic activity and high performances in degradation of methylene blue under visible light irradiation and could, therefore, be reused at least five times, with only a slight decrease in photocatalytic activity. In addition, this catalyst could be easily separated at the end of the reaction using centrifuging. The results showed that supported catalyst could accelerate electron transfer in photocatalytic procedures due to good dispersion of NiOAC on the surface of modified graphene nanosheets.

Acknowledgement

The authors are thankful from Payame Noor University in Isfahan Research Council and contributions from Brijand University are gratefully acknowledged.

References

- [1] Soldano C., Ather M., Erik D. *Carbon*. 2010, **8**:2127
- [2] Kuila T., Mishra A.K., Khanra P. *Prog. Mater. Sci.*, 2012, **57**:1061
- [3] Dreyer D.R., Park S. *Chem. Soc. Rev.*, 2010, **1**:228
- [4] Compton O.C., Nguyen S.T. *Small.*, 2010, **6**:711
- [5] Varghese N., Mogera U., Govindaraj A. *Chem. Phys. Chem.*, 2009, **10**:206
- [6] Tang L.H., Wang Y., Liu Y. *Acs. Nano.*, 2011, **5**:3817
- [7] W.Lv, M.Guo, M. H.Liang, F. M.Jin, L.Cui, L. Zhi,Q. H.Yang, J Mat Chem20, **2010**, 32, 6668.
- [8] Ferri T., Frasca D. *Angew. Chem. Int. Ed.*, 2011, **50**:7074
- [9] Su Q., Pang S.P., Alijani V. *Adv. Mater.*, 2009, **21**:3191
- [10] Zhu Y., Murali S., Cai W., Li X., Suk J.W. *Adv. Mater.*, 2010, **22**:3906
- [11] Hsu H.C., Shown I. *Nanoscale*, 2013, **5**:262
- [12] Liu S., Tian J., Wang L., Luo Y., Sun X. *Catal. Sci. Technol.*, 2012, **2**:339
- [13] Chen G., Sun M., Wei Q., Zhang Y., Zhu B. *J. hazard. Mater.*, 2013, **244**:86
- [14] Pastrana-Martínez L.M., Morales-Torres S., Likodimos V., Figueiredo J.L., Faria J.L., Falaras P., Silva A.M. *Appl. Catal. B: Environ.*, 2012, **123**:241
- [15] Kim S.P., Choi H.C. *Bull. Korean Chem. Soc.*, 2014, **9**:2661
- [16] Yang X., Chen W., Huang J., Zhou Y., Zhu Y., Li C. *Scientific reports*, 2015, **5**
- [17] Daniela C. *Acs. Nano.*, 2010, **4**:4806

- [18] Huang J., Zhang L., Chen B., Ji N. *Nanoscale*, 2010, **2**:2733
- [19] Scheuermann G.M., Rumi L., Steurer P. *J. Am. Chem. Soc.*, 2009, **131**:8262
- [20] Chakravarty A., Bhowmik K. *Langmuir*, 2015, **31**:5210
- [21] Stein M., Wieland J., Steurer P., Tolle F. *Adv. Synth. Catal.*, 2011, **353**:523
- [22] Stankovich S., Dikin D.A., Dommett G.H. *Nature*, 2006, **442**:282
- [23] Ramanathan T., Abdala A.A., Stankovich S. *Nat. Nanotechnol*, 2008, **3**:327
- [24] Lee Y.R., Raghu A.V., Jeong H.M., Kim B.K. *Macromol. Chem. Phys.*, 2009, **210**:1247
- [25] Tjong S.C. *Energy. Env. Sci.*, 2011, **4**:605
- [26] Chiacchiarelli L.M., Rallini M., Monti M. *Compos. Sci. Technol.*, 2013, **80**:73
- [27] Ren L., Qiu J., Wang S. *Smart. Mater. Struct.*, 2012, **21**:105
- [28] Chen Y., Qi Y., Tai Z., Yan X., Zhu F., Xue Q. *Eur. Polym. J.*, 2012, **48**:1026
- [29] Ghosh A., Sinha K., Das Saha P. *Destalination. Water. Treat.*, 2013, **51**:7791
- [30] Mansourpanah Y., Shahebrahimi H., Kolvari E. *Chem. Engin. Design.*, 2015, **104**:530
- [31] Hanawalt, *Anal. Chem.*, 1938, **10**:475
- [32] Liu S., Tian J., Wang L., Luo Y., Sun X. *Catal. Sci. Tech.*, 2012, **2**:339

How to cite this manuscript: Mehrnaz Alem, Abbas Teimouri*, Hossein Salavati*, Shahnaz Kazemi. Central composite design optimization of methylene blue scavenger using modified graphene oxide based polymer. *Chemical Methodologies* 1(1), 2017, 49-67. DOI: [10.22631/chemm.2017.49743](https://doi.org/10.22631/chemm.2017.49743).